

מכון ויצמן למדע

WEIZMANN INSTITUTE OF SCIENCE



## STUDIES ON THE EARLY STAGES OF CRYSTAL NUCLEATION

### Document Version:

Publisher's PDF, also known as Version of record

### Citation for published version:

Popovitz-Biro, R, Weissbuch, I, Jacquemain, D, Leveiller, F, Leiserowitz, L & Lahav, M 1991, STUDIES ON THE EARLY STAGES OF CRYSTAL NUCLEATION. in *Advances in industrial crystallization*. WTI-Frankfurt-digital GmbH, pp. 3-19.

*Total number of authors:*

6

### Published In:

Advances in industrial crystallization

### License:

Other

### General rights

@ 2020 This manuscript version is made available under the above license via The Weizmann Institute of Science Open Access Collection is retained by the author(s) and / or other copyright owners and it is a condition of accessing these publications that users recognize and abide by the legal requirements associated with these rights.

### How does open access to this work benefit you?

Let us know @ [library@weizmann.ac.il](mailto:library@weizmann.ac.il)

### Take down policy

The Weizmann Institute of Science has made every reasonable effort to ensure that Weizmann Institute of Science content complies with copyright restrictions. If you believe that the public display of this file breaches copyright please contact [library@weizmann.ac.il](mailto:library@weizmann.ac.il) providing details, and we will remove access to the work immediately and investigate your claim.

## Rapid #: -18686494

CROSS REF ID: **5694990140003596**

LENDER: **JSL :: Main Library**

BORROWER: **I9W :: Main Library**

TYPE: Book Chapter

BOOK TITLE: Advances in industrial crystallization

USER BOOK TITLE: Advances in industrial crystallization

CHAPTER TITLE: STUDIES ON THE EARLY STAGES OF CRYSTAL NUCLEATION

BOOK AUTHOR: Garside, R. J. Davey, A. G. Jones

EDITION:

VOLUME:

PUBLISHER:

YEAR: 1991

PAGES: -

ISBN: 9780750611732

LCCN:

OCLC #:

Processed by RapidX: 2/21/2022 8:21:18 AM

---

This material may be protected by copyright law (Title 17 U.S. Code)

---

## STUDIES ON THE EARLY STAGES OF CRYSTAL NUCLEATION

R Popovitz-Biro, I Weissbuch, D Jacquemain, F Laveiller, L Leiserowitz and M Lahav

Department of Structural Chemistry,  
The Weizmann Institute of Science, Rehovot,  
ISRAEL

### INTRODUCTION

The understanding of dynamics of the phase transformation from a supersaturated solution into a crystalline solid, requires knowledge of the solution structure at the onset of crystallization. Indication for the existence of large molecular clusters in supersaturated solutions was presented by the pioneering studies of Mullin and Leci [1]. The authors reported that isothermal columns of supersaturated solutions of citric acid developed concentration gradients. Larson and Garsides [2,3] obtained similar results for aqueous solutions of electrolytes ( $\text{NaNO}_3$ ,  $\text{K}_2\text{SO}_4$ ) and non-electrolytes (urea). The phenomenon was explained by assuming the formation of molecular clusters in the size range of 4-10 nm ( $10^3$  molecules). Khamskii [4] reported that light transmission through supersaturated solutions decreased continuously prior to the onset of crystallization. Meyerson et al. [5] determined the diffusion coefficients of various solutes in concentrated and saturated solutions using Gouy interferometry. The observed decrease in the diffusion coefficient with increase of concentration implied once again the formation of aggregates in the supersaturated solution. While these macroscopic methods provide important experimental proof for the existence of clusters at the onset of crystal nucleation, they, however, yield little information on the structure of these clusters and the role they play as intermediates in the crystallization process.

We shall discuss here a complementary approach which is stereochemical in nature to provide knowledge on the molecular level, on the structure, dynamics of growth and dissolution in different environments of these clusters. The methodologies applied include oriented crystallization at the air/solution interface as a tool for detecting and

probing the structure of molecular clusters of insoluble and soluble amphiphiles. The packing arrangement and the orientation of the molecules within some of the clusters have been determined using the methods of grazing incidence X-ray diffraction (GIXD), and second harmonic generation (SHG). Time resolved aggregation in two-dimensions of some surfactants has been also monitored by the GIXD technique. The stereochemical approach has been used for the design of "tailor-made" polymers as additives to control crystal polymorphism and resolution of enantiomers by crystallization.

## EPITAXIAL CRYSTALLIZATION UNDER AMPHIPHILIC MOLECULES

### Oriented crystallization of $\alpha$ -glycine by soluble hydrophobic $\alpha$ -amino acids [6.7]

The crystalline structure of the monoclinic  $\alpha$ -form of glycine is composed of hydrogen bonded layers in which the molecules are related in the  $ac$  plane by translation symmetry only (Fig.1). The area per molecule within such a layer is  $ac \sin\beta = 25.9\text{\AA}^2$ . The layers are interlinked by N-H...O bonds via centers of inversion to form centrosymmetric bilayers. Since each layer is chiral, the replacement of the C-H group of glycine molecule, which emerges from the (010) crystal surface, by an alkyl



Figure 1 Packing arrangement of  $\alpha$ -glycine viewed : a) perpendicular to the  $a c$  layer of molecules; b) along the  $a$  axis, displaying the bilayer of molecules.



group for example, would generate a chiral  $\alpha$ -amino acid surface layer of *R*-configuration. By virtue of the glide or inversion symmetry of the crystal, a layer of glycine molecules at the opposite ( $0\bar{1}0$ ) crystal surface may be replaced by a chiral layer of (*S*)- $\alpha$ -amino acids.

The hydrophobic optically pure  $\alpha$ -amino acids valine, leucine, norleucine, isoleucine, phenylalanine and  $\alpha$ -amino octanoic acid, all pack in hydrogen-bonded layer structures similar to that of  $\alpha$ -glycine. The area per molecule within each layer ranges from 25.1 to 26.6 Å<sup>2</sup>, close to that of  $\alpha$ -glycine. Surface tension measurements of aqueous solutions of these amphiphilic molecules, both pure as well as saturated in glycine, indicated a positive surface accumulation parameter, implying that these molecules aggregate at the solution surface. It is our hypothesis that the molecules at the surface may form ordered 2-D aggregates stabilized by the hydrogen bonds formed between their polar head groups. The proof for this proposed lateral ordering involved the design of structured surfaces which may act as a template at the air/solution interface for an epitaxial like crystallization of 3-D crystals such as glycine .

With this idea in mind, we investigated the oriented crystallization of glycine in the presence of low concentrations of optically pure hydrophobic  $\alpha$ -amino acids. We took advantage of the fact that one class of the hydrophobic  $\alpha$ -amino acids form crystalline layer structures similar to that of glycine, while the other class was selected so that its hydrophobic moieties are too bulky to allow the formation of a similar layer structure. Indeed, the crystal packing arrangements of compounds such as *t*-butyl glycine and neopentyl glycine show the formation of a hydrogen-bonded layer that occludes solvate water since the bulky hydrophobic groups impose too large separation distances between neighbouring molecules (Fig.2). Consequently, we expected that only the first class of  $\alpha$ -amino acids, used in minor concentrations as cosolutes can induce an oriented crystallization of glycine at the air/solution interface. The *R*- $\alpha$ -amino acids should trigger glycine nucleation from the (010) face and the *S*- $\alpha$ -amino acids from the ( $0\bar{1}0$ ) face. Indeed, addition of as little as 0.1-1% of the optically pure hydrophobic  $\alpha$ -amino acid induced a fast oriented crystallization at the interface . In contrast, as expected, addition of  $\alpha$ -amino acids with bulky side chains, such as *t*-butyl glycine, neopentyl glycine, or hexafluorovaline did not induce  $\alpha$ -glycine crystallization at the solution surface. The oriented nucleation does not occur despite the high aggregation of additive at the air/solution interface which was determined from surface tension measurements. This result is in keeping with a mismatch between the proposed

2-D packing of the bulky  $\alpha$ -amino acids at the water surface and the layer structure of glycine.

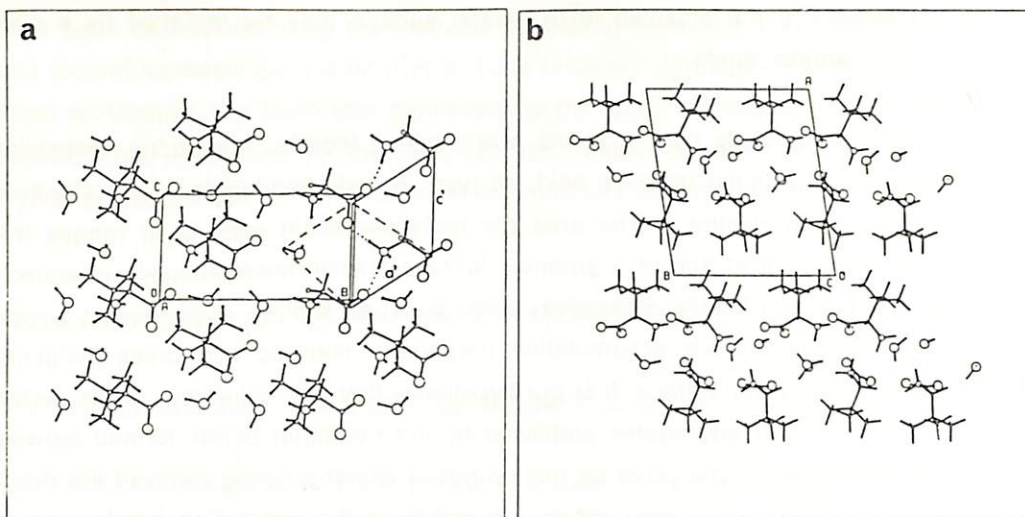


Figure 2 Packing arrangement of (S) t-butyl glycine monohydrate crystal viewed : a) perpendicular to the layer of molecules; b) along the *c* axis. The water molecules form strands separating the ribbons of *t*-butyl glycine molecules.

#### Oriented crystallization of $\alpha$ -glycine under $\alpha$ -amino acid monolayers [8,9]

In order to obtain more direct information on the structure of molecular aggregates formed at the air/solution interface, we extended our studies on the induced crystallization of glycine by insoluble amphiphilic  $\alpha$ -amino acids. These surfactant molecules, in contrast to the short chain  $\alpha$ -amino acids, are amenable to surface analysis such as surface pressure-area isotherms. Only very recently, with the advent of intense, highly collimated and monochromatic X-ray beams from synchrotron sources, it became possible (in cooperation with K. Kjaer and J. Als-Nielsen) to probe the structure of the crystalline domains formed by these amphiphiles at the air/solution interface. Crystallization experiments of glycine underneath amphiphilic molecules with a surface molecular area of  $\sim 25\text{\AA}^2$ , close to that of glycine at the {010} face, yield results akin to that of the corresponding hydrophobic  $\alpha$ -amino acids. This behaviour is expressed both for the compressed or non-compressed monolayer. Thus, for example, monolayers of palmitoyl-*R*-lysine, stearyl-*R*-glutamate yield complete oriented crystallization of glycine. On the other hand, optically pure  $\alpha$ -amino

acid monolayers which bear a fluorocarbon tail, imposing a molecular area of  $28.5\text{\AA}^2$ , induce crystallization of glycine with both (010) and (0 $\bar{1}$ 0) orientations. An  $\alpha$ -amino acid monolayer with a bulky steroid side chain of surface molecular area of  $38\text{\AA}^2$  does not induce, as expected, crystallization of glycine. The structure of two of these monolayers was determined by GIXD measurements .

Figure 3 depicts the experimental in-plane diffraction pattern obtained from the palmitoyl-*R*-lysine monolayer [10]. The monolayer proved to be a 2-D powder with a "coherence length" (in other words, a perfect crystalline domain size) of about  $500\text{\AA}$  and unit cell dimensions  $a=5.03$ ,  $b=5.46\text{\AA}$ ,  $\gamma=117.8^\circ$ , implying a molecular area of  $24.3\text{\AA}^2$ . The molecular layer thickness was determined from X-ray reflectivity measurements and compares well with that provided by the molecular model deduced from the GIXD data and X-ray powder diffraction data of 3-D crystalline palmitoyl-*R*-lysine. It was deduced that the hydrophobic chain axis of the monolayer molecule is tilted by  $30^\circ$  from the vertical, such an orientation being favorable for hydrogen-bonding between neighbouring amide groups (Fig 4). These bonds fix the chain

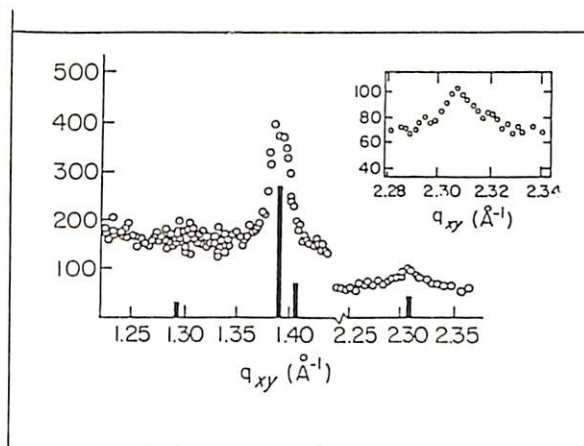


Figure 3 GIXD in-plane diffraction pattern of the palmitoyl-*R*-lysine monolayer.

orientation and packing. On these bases, a model was proposed (Fig. 4) in which the packing arrangement of the  $\alpha$ -amino acid head groups is very similar to that of an *ac* layer of glycine in its own crystal structure. We propose that this similarity in packing arrangement is responsible for the epitaxial crystallization of glycine at the air/solution interface. In contrast, GIXD data for the fluorinated  $\alpha$ -amino acid  $\text{CF}_3(\text{CF}_2)_9(\text{CH}_2)_4\text{OCOCH}_2\text{CH}(\text{NH}_3^+)\text{CO}_2^-$  (PFA) in the compressed state yielded a cell



which differs significantly from that of  $\alpha$ -glycine [11]. Attempts to observe in-plane diffraction at room temperature of uncompressed monolayer of palmitoyl-*R*-lysine was unsuccessful. Nevertheless, uncompressed monolayer of the fluorinated  $\alpha$ -amino acid PFA at room temperature [12] and amphiphiles such as alcohols, acids and amides at low temperature form crystalline clusters according to GIXD measurements [13].

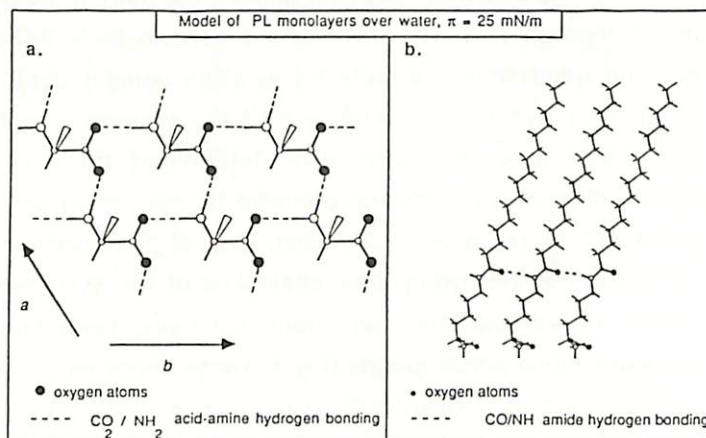


Figure 4 Model of the palmitoyl -*R* - lysine monolayer packing arrangement viewed : a) perpendicular to the layer; b) 'edge-on'.

#### Growth of 2-D PFA crystallites monitored by GIXD [12]

The grazing incidence X-ray diffraction technique provides an analytical tool to study time-resolved crystallization of amphiphilic molecules in two dimensions. Time-resolved GIXD measurements of the growth of PFA crystallites on pure water at room temperature were not feasible because the measuring time was too long compared to the time required for crystalline self-aggregation. On the other hand, growth of crystallites over a solution of glycine was substantially impeded so that crystallite formation could be monitored in real time. Ten minutes after deposition of the surfactant, no GIXD signal could be detected. The integrated peak intensity reached a plateau about 50 minutes after deposition (Fig.5), implying a saturation of the number of ordered molecules; the coherence length took more time (150 minutes) to reach a value  $\geq 1500\text{\AA}$ . These studies might provide some clues on aging of supersaturated solutions before crystallization begins, a process which has been inferred for many organic and inorganic materials.



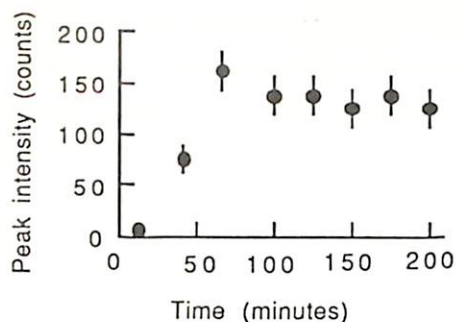


Figure 5 Integrated peak intensity of PFA on glycine subphase as a function of time .

### Crystallization of NaCl under monolayers [14]

In the  $\alpha$ -amino acid surfactant/glycine system, the polar head groups of the molecules in the 2-D aggregates at the air/solution interface may be regarded as forming the first layer of the to-be-grown glycine crystal. In principle, one may extend this approach for designing surfaces which will induce organization of layers of atomic or molecular ions in solution. Such structured ionic layers may be similar or complementary to the layer structure of the to-be-nucleated crystal. In order to probe the feasibility of this approach, we studied the nucleation of sodium chloride underneath several monolayers at different pH values [12].

Sodium chloride precipitates from aqueous solutions in the cubic space group  $Fm\bar{3}m$ ,  $a=5.64\text{\AA}$ , exhibiting six  $\{100\}$  crystal faces. When crystallized under specific conditions, two other less stable faces  $\{110\}$  and  $\{111\}$  can be expressed. The  $\{110\}$  face (Fig. 6a) is composed of alternating rows of  $\text{Na}^+$  and  $\text{Cl}^-$  ions, separated by  $2.82\text{\AA}$ . On the other hand, the  $\{111\}$  face is composed of ions of the same kind (i.e.,  $\text{Na}^+$  or  $\text{Cl}^-$ ) (Fig 6b). The juxtaposed layers of opposite charge neutralize the system.

When monolayers of arachidic or stearic acid were spread over NaCl solution, 70-90% of the sodium chloride crystals nucleated from their  $\{111\}$  faces. Since the 111 layer is comprised of ions of one type only, were the  $\text{Na}^+$  ions aligned underneath a layer containing carboxylate head groups, they would, in an ordered system, pack in an identical hexagonal net in order to conserve charge neutrality. The hexagonal lattice of the  $\{111\}$  face of NaCl is  $a'=b'=3.99$ ,  $\gamma'=120^\circ$ , with an area of  $14.5\text{\AA}^2$ . Thus, there can be no structural match between the layer of  $\text{Na}^+$  ions attached to the monolayer with

an area/molecule of approximately  $20\text{\AA}^2$  and the underlying 111 layer of  $\text{Cl}^-$  ions of area  $14.5\text{\AA}^2$ . Thus, the observation that up to 90% of the NaCl crystals are attached with their {111} faces to the monolayer may be explained by electrostatic attractions. Amphiphilic acids, with a large surface area per molecule, such as cholesteryl succinate ( $\sim 38\text{\AA}^2$ ), do not induce crystallization of NaCl at all. This is in keeping with the expectation that the double layer of  $\text{Na}^+$  ions below the carboxylate layer is more diffuse, thus reducing the chance for induced nucleation of NaCl attached with its {111} face at the interface.

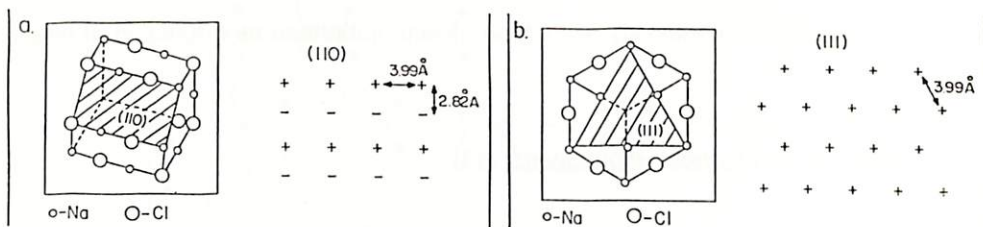


Figure 6 Schematic representation and point charge distribution of: a) the {110} face ;b) the {111} face of NaCl crystal.

Monolayers of zwitterionic  $\alpha$ -amino acids, in the pH range of 3 to 10, induce a fast nucleation of NaCl. At neutral pH, many NaCl crystals nucleate from the {110} face. We may account for the preference of the {110} face on the following grounds: the distribution of  $\text{Na}^+$  and  $\text{Cl}^-$  ions at the {110} face of NaCl and that of the  $\text{NH}_3^+$  and  $\text{CO}_2^-$  moieties of the polar head groups of the monolayer are complementary to one another. The distance between adjacent rows of  $\text{Na}^+$  and  $\text{Cl}^-$  ions on the {110} face is  $2.82\text{\AA}$  (Fig. 6) matching fairly well the  $2.6\text{\AA}$  separation distance between adjacent rows of  $\text{NH}_3^+$  and  $\text{CO}_2^-$  moieties in the monolayers.

A systematic study has been carried out on the induced crystallization of NaCl by PFA at different pH values. At neutral pH, the monolayer induces crystallization of NaCl from the {110} face and at  $\text{pH} > 11.1$ , from the {111} face. We could deduce that the  $\text{Na}^+$  ions bound to the anionic  $\text{H}_2\text{N-CH-CO}_2^-$  head groups of the monolayer expose to the solution an equipotential ionic layer suitable for NaCl nucleation. GIXD studies of PFA monolayers spread over highly basic KOH subphases ( $\text{pH}=11.5$ ) yielded results in favour of a laterally ordered PFA- $\text{K}^+$  bilayer. The study was carried out with  $\text{K}^+$  ions which are stronger X-ray scatterers than  $\text{Na}^+$  ions. The presence of  $\text{K}^+$  ions induces all PFA molecules to be assembled into 2-D crystals, even in the uncompressed state, with

the molecules aligned vertically in a hexagonal cell (Fig. 7 ). The  $K^+$  ions probably occupy ordered sites, bridging oxygen atoms of neighbouring molecules, (Fig. 7a) and are hydrated with one water molecule per head group.

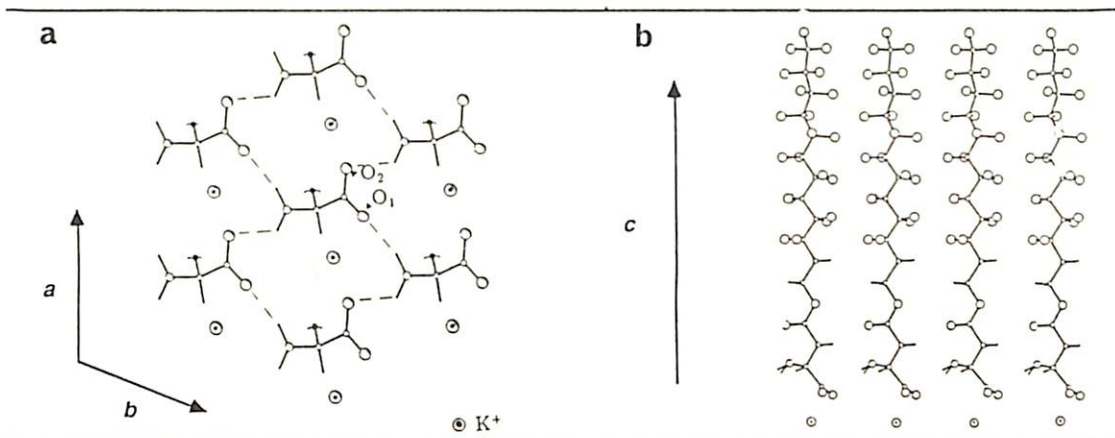


Figure 7 Model arrangement of PFA molecules in self-assembled crystallites at high pH : a) view along  $c$  axis ; b) view along  $a$  axis . The attached layer of  $K^+$  ions is shown.

The epitaxial growth of 3-D crystals of NaCl from their  $\{110\}$  face in acidic pH can be explained by intercalation of  $Cl^-$  ions between positively charged  $^+H_3N-CH-COOH$  head groups (Fig. 8). Comparative GIXD studies on perfluorinated monolayers in the uncompressed state at different pH values, demonstrated a measurable increase in the surface area per molecule; at acidic pH  $31.6\text{\AA}^2$  instead of  $28.5\text{\AA}^2$  at high pH.

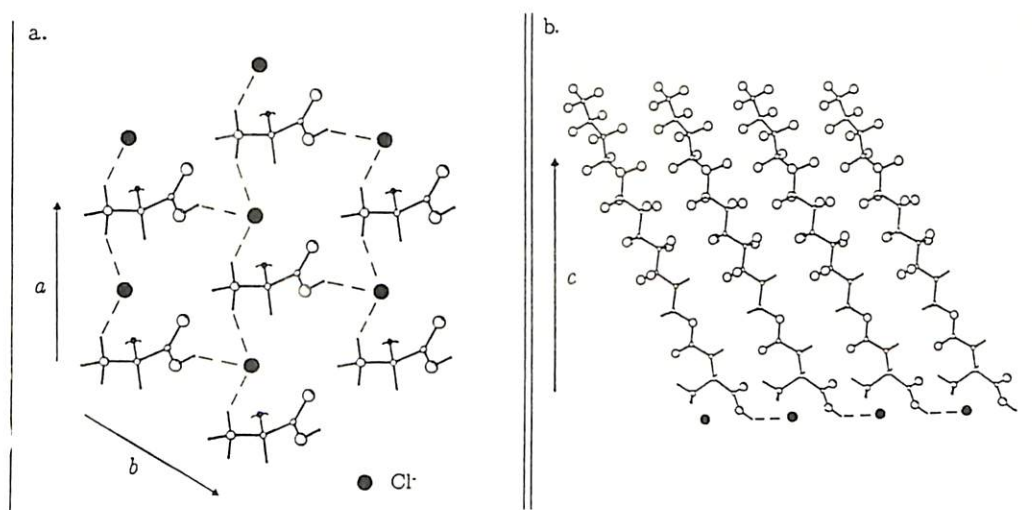


Figure 8 Model arrangement of PFA molecules in self-assembled crystallites at low pH a) view along  $c$  axis ; b) view along  $a$  axis. The attached layer of  $Cl^-$  ions is shown.



Supporting evidence is obtained from the packing arrangement of 3-D crystals of glycine.HCl and valine.HCl. In each layer of these crystals, the positively charged  $\alpha$ -amino acid molecules are related by translation and are interlinked by  $\text{Cl}^-$  ions forming hydrogen bonded nets with a repeat molecular area of  $36\text{-}37\text{\AA}^2$ . Since the repeat area in the PFA monolayer at low pH is only  $31.6\text{\AA}^2$ , this implies that the  $\text{Cl}^-$  ions cannot intercalate completely in the monolayer plane but probably lie about  $1\text{\AA}$  below it, linking two  $\text{NH}_3^+$  and one  $\text{CO}_2\text{H}$  moieties (Fig.8). We note here that the positive unit charge of the  $\text{NH}_3^+$  is probably distributed equally amongst the three hydrogen atoms and the amino groups are arranged so that there is no short intermolecular distance between their hydrogen atoms.

#### Induced nucleation of ice by alcohols [15]

Pure water can be supercooled to temperatures of  $-20^\circ\text{C}$  to  $-40^\circ\text{C}$ . Therefore the induction or inhibition of freezing of ice, in particular through the role of auxiliaries, such as membranes or proteins, has far reaching ramifications for the living and non-living world. Water-soluble alcohols generally reduce the freezing point of water. In contrast, we expected that insoluble amphiphilic alcohols at the air/water interface might form 2-D crystalline domains with structure akin to that of hexagonal ice and thus act as ice nucleators. This expectation was based on GIXD studies of a compressed monolayer of heneicosanol ( $\text{C}_{21}\text{H}_{43}\text{OH}$ ) at the air/water interface carried out by Dutta, Rice and coworkers [16]. The unit cell of the crystalline monolayer at temperatures just above  $0^\circ\text{C}$ , is distorted hexagonal with axes  $a=b=4.5\text{\AA}$ ,  $\gamma=113^\circ$ , and area per molecule  $a^2\sin\gamma=18.6\text{\AA}^2$ . Thus the arrangement of the OH head groups of the alcohol at the water surface would appear to mimic or complement the (001) face of hexagonal ice since the ice has unit cell dimensions  $a=b=4.5\text{\AA}$ ,  $\gamma=120^\circ$  (Fig. 9). The proposed structural match between the monolayer and the layer of ice in the  $ab$  plane, suggested that such monolayers should be efficient nucleators of ice. Nucleation efficiencies could be evaluated by measuring the freezing points of supercooled water drops covered by such monolayers. Freezing point measurements were carried out on water drops of the same size (ranging from  $10$  to  $40\ \mu\text{l}$ ) placed on a cooling stage in a box purged by cold nitrogen gas. Comparative measurements were done using the alcohols and the corresponding acid as a reference. The freezing point measurements showed that the aliphatic chain alcohols nucleate ice at higher temperatures and with greater reproducibility than the analogous acids (Fig. 10). The freezing point is sensitive to



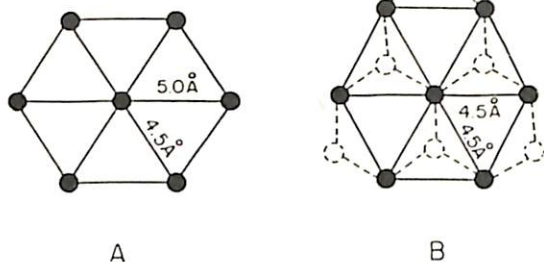


Figure 9 Schematic representation of  
 A) A distorted hexagonal lattice of heneicosanol on water; B) The lattice of hexagonal ice viewed along the  $c$  axis.

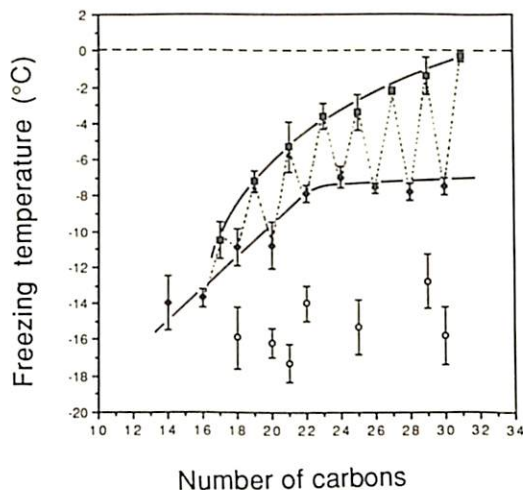


Figure 10 Freezing points of supercooled water drops covered by monolayers of alcohols  $C_nH_{2n+1}OH$  ( $n$  odd ■,  $n$  even ◊) and carboxylic acids  $C_{n-1}H_{2n}CO_2H$  (○).

the length and parity of the chain. The curve for the  $n$ -odd series increases asymptotically with chain length approaching  $0^\circ\text{C}$  for  $n=31$ . The  $n$ -even series behave differently; the freezing point curve reaches a plateau of about  $-8^\circ\text{C}$  for  $n$  in the range 22 to 30.

We recently performed GIXD measurements on several monolayer alcohols ( $n=23,30,31$ ) and on one acid ( $n=30$ ) over pure water at  $5^\circ\text{C}$ [12]. The measurements were made in the uncompressed state at  $\sim 70\%$  surface coverage. Diffraction peaks observed for all films indicated the formation of self-aggregated crystalline domains with anisotropic coherence lengths of  $\sim 300$  and  $\sim 1000\text{\AA}$ . The cell dimensions (Table 1) show a good lattice match between the  $ab$  lattice of ice and the lattices of the alcohols but not with the acid monolayer. This structural fit is probably responsible for the efficient ice nucleation by the alcohols. However, we cannot account for the observed differences in ice nucleation from the minor differences in cell dimensions and molecular tilt angles between the various odd and even alcohols.

Table 1. Cell Constants of Uncompressed Monolayers over Pure Water at 5°C

Monolayer	$a = b$ (Å)	$\gamma$ (°)	area= $a^2 \sin \gamma$ (Å <sup>2</sup> )	Molecular tilt angle
C <sub>23</sub> H <sub>47</sub> OH	4.54	113.0	18.9	10°
C <sub>30</sub> H <sub>61</sub> OH	4.50	112.8	18.7	8°
C <sub>31</sub> H <sub>63</sub> OH	4.52	113.1	18.8	11°
C <sub>29</sub> H <sub>59</sub> CO <sub>2</sub> H	4.65	106.3	20.6	26°

Recently, ice nucleation studies have been extended to various mixed monolayers as well as to the effect of the amphiphilic alcohols at the liquid/liquid interface.

#### Oriented crystallization of *p*-Hydroxybenzoic Acid by *p*-alkoxy derivative [17]

*p*-Hydroxybenzoic acid (HBA) monohydrate crystallizes from pure aqueous solutions as elongated plate-like crystals, usually at the bottom of the crystallizing dish. Addition of 5% (wt/wt) *p*-methoxybenzoic acid (MBA) to the solution induces fast nucleation of the crystals floating at the air/solution interface. These crystals nucleate and appear attached at the interface via a newly expressed (401) face. Insoluble amphiphilic molecules like *p*-alkoxy- and *p*-alkylamino benzoic acids also induce the (401) oriented crystallization of HBA.

Our proposed mechanism which can explain the induced epitaxial crystallization, is based on a structural match between the (401) crystalline face and that of aggregates of additive molecules formed at the interface (Fig. 11). Thus, we have to assume that the hydrophobic MBA molecules which adsorb and form aggregates at the air/solution interface, must lie with their aromatic moieties parallel to the interface which, at first glance, appeared to be counter-intuitive.

In order to shed light on the surface orientation both of insoluble amphiphiles and MBA,

we made use of SHG spectroscopy (in cooperation with G. Berkovic). Such surface sensitive measurements demonstrated that while on pure water subphase the polarizable moieties of the amphiphiles are oriented almost perpendicular to the surface (tilt angle relative to the normal of  $24\text{-}42^\circ$ ), upon addition of *p*-hydroxy benzoic acid to the subphase, the SHG signal vanishes.

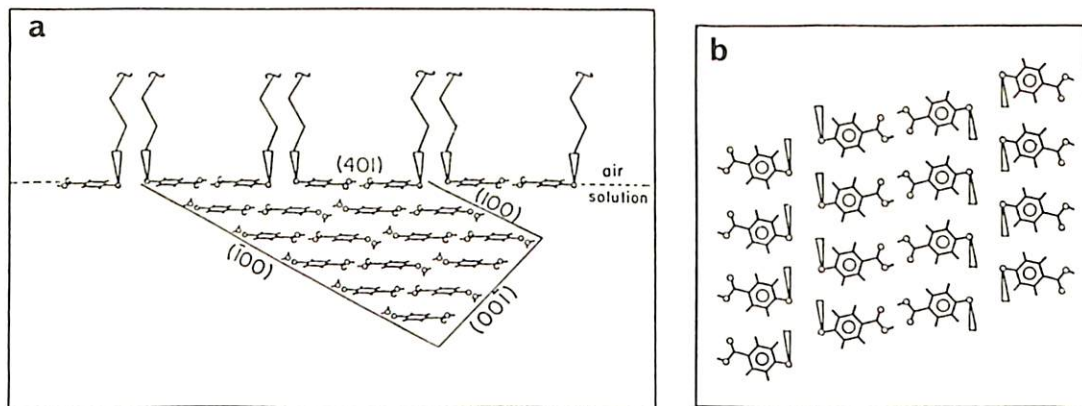


Figure 11 a) Packing arrangement of *p*-hydroxybenzoic acid monohydrate crystal with the (401) face attached at a monolayer/solution interface viewed 'edge-on'. b) Proposed model of the amphiphilic molecules at the interface, viewed perpendicular to the (401) face.

One reasonable way to explain this effect is to assume that on the *p*-hydroxybenzoic acid subphase, the amphiphilic molecules assume an orientation such as their  $\text{HOOC}-\Phi-\text{O}-$  moiety ( $\Phi$ =aromatic ring) is parallel to the solution surface forming hydrogen bonded centrosymmetric carboxylic acid pairs (Fig. 11b). This arrangement is in agreement with the expression of the (401) face by which the HBA crystals grow attached to the interface. The dramatic change in orientation of the amphiphiles is induced by strong interactions with the *p*-hydroxybenzoic acid molecules and is very specific to the nature of the solute molecules. Indeed, such a change did not occur with subphase containing *p*-hydroxyphenylacetic or cinnamic acids.



## "TAILOR - MADE" POLYMERS FOR THE CONTROL OF POLYMORPHISM

Structured clusters may form not only at air/solution interfaces but also at glass/solution interfaces or even in the bulk of supersaturated solutions. However, since the analytical tools amenable to the "smooth" air/water interface, are not yet applicable for the "rough" solid/solution interface or the bulk of the solution, we made use of indirect methods. In one of these approaches, we used as a working hypothesis, the assumption that nuclei of precritical size adopt structures akin to those of mature crystals into which they evolve. This methodology was instrumental in the design of polymers for the resolution of conglomerates[18, 19].

More recently, together with L. Addadi and E. Staab, we took this hypothesis a step further, assuming that supersaturated solutions of materials displaying polymorphism may contain molecular aggregates of structures resembling those of the various mature phases. Under conditions close to equilibrium, however, only the nuclei corresponding to the thermodynamically stable phase, grow into crystals. A properly designed inhibitor should preferentially interact with precritical nuclei of the stable crystalline phase, and much less, if at all, with those of the desired metastable one. The strong inhibition of the stable phase will lead to preferential precipitation of the thermodynamically metastable polymorph by virtue of kinetic control. Modelling the inhibitor molecule is based on the analysis of the crystal packing arrangement of the various polymorphs. This approach was successfully applied for crystallization of a metastable polar polymorph on the expense of the stable quasi-centrosymmetric one [20].

N-(2-acetamido-4-nitrophenyl)pyrrolidene, PAN, exists in two distinct crystalline forms. Form  $\alpha$  is quasi-centrosymmetric and is generally obtained as thick plates, either by slow cooling or slow evaporation. On the other hand, when aqueous solutions of PAN are cooled rapidly, a metastable  $\beta$ -form precipitates as dendritic needles. Upon standing in solution or heating to 183-186°C, the needles transform into plates of the stable  $\alpha$ -form. The packing arrangement of the two structures are shown in Figure 12. In the  $\alpha$ -form, the acetamido groups of the two independent molecules are antiparallel and so oriented towards the  $+b$  and  $-b$  directions, while in the polar  $\beta$ -form the symmetry related molecules have the same component of the acetamido group oriented



exclusively towards one direction along the  $b$ -axis, say  $+b$ . In both systems the acetamido group has also components along the  $c$ -axis.

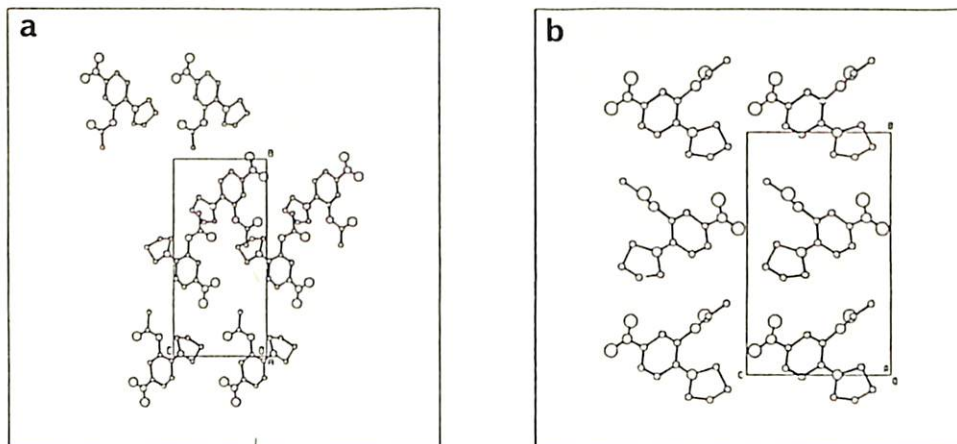


Figure 12 Packing arrangement of the PAN crystals : a) non-polar  $\alpha$ -form viewed down the  $a$  axis ; b) metastable polar  $\beta$ - form viewed down the  $a$  axis.

On the basis of the information from the two crystal structures, and of our previous knowledge on the mode of operation of "tailor-made" inhibitors, we predicted that substitution of acetamido groups with a different moiety 'X', will generate efficient crystallization inhibitors. These molecules should adhere to both nuclei of the  $\alpha$ - and the  $\beta$ -form; however, they should be adsorbed and consequently slow down the growth of crystals and nuclei of  $\alpha$ -form from the  $+b$ ,  $-b$  and  $c$  directions. Analogously, they should inhibit the growth of  $\beta$ -form crystals and nuclei along  $c$ , but only from one of the two directions along  $b$ . We thus expected that in the presence of such an inhibitor, nuclei of the  $\alpha$ -form would be preferentially prevented from growing. It has been recently shown that soluble polymeric additives when used as nucleation inhibitors, are superior by orders of magnitude than the corresponding monomeric ones because of the cooperative binding to the to-be-affected surface. Thus, grafting the monomeric units to a polymer backbone, yield more efficient auxiliaries. Indeed, soluble polymeric additives composed of PAN grafted to polyacrylic and polymethacrylic acids are most effective inhibitors (0.03% wt/wt) of the stable  $\alpha$ -polymorph.

## OUTLOOK

Recent availability of several analytical tools has opened new ways to obtain direct insight into the structure, size and shape of clusters functioning as nucleation intermediates at the onset of crystallization. Grazing incidence X-ray diffraction using synchrotron radiation has provided important information regarding the structure of 2-D clusters. So far such GIXD measurements were carried out on 2-D "powders" of surfactants at air/water interfaces. But with advances in synchrotron technology, it may soon be possible to obtain diffraction spectra from "single crystals" of Langmuir films and so provide direct structural information at atomic resolution.

We may anticipate an extension of these studies to the bulk of supersaturated solutions, which will provide knowledge on the structure of 3-D clusters and the effect of the environment on them. GIXD also provides an entry into the packing of ions and molecules in the "liquid" layer directly attached to the Langmuir film. Recently, diffraction peaks were obtained from a layer of  $\text{Cd}^{2+}$  ions forming part of an uncompressed layer of Cadmium arachidate at high pH. Fourteen diffraction peaks were observed from this monolayer, seven of which were attributed to only the  $\text{Cd}^{2+}$  layer [21], from which the  $\text{Cd}^{2+}$  positions could be calculated. The relevance of these structured layer of ions and perhaps interleaving water molecules might shed light on the early stages of crystal nucleation.

Most of the GIXD studies have been carried out at the "smooth" air/water interface but it should become possible in the not too distant future to determine the structure and the size of clusters growing also from solid/liquid interfaces. Such a knowledge should remove many of the unknowns associated with the process of crystal nucleation.

**Acknowledgements** We thank L. Addadi, G. Berkovic, K. Kjaer and J. Als-Nielsen for fruitful cooperation and many discussions; E. Shavit for synthesis of many of the surfactants used in this work; the US/Israel Binational Foundation, Jerusalem and the donors of the Petroleum Research Fund of the American Chemical Society, for financial support.

## REFERENCES

1. Mullin, J W, and Leci, C, Philos Mag (1969) 19 1075
2. Larson, M A and Garside, J, J of Cryst Growth (1986) 76 88
3. Larson, M A and Garside, J, J Chem Eng Sci (1986) 41 1285
4. Kamskii, E V, "Crystallization from solution" Consultant Bureau, NY, (1969)
5. Myerson, A S, Lo, P Y, Kim, Y C, Ginde, R in "Proceedings of the 11<sup>th</sup> Symposium in Industrial Crystallization" L-23, (1990), A.Mersman Editor.
6. Weissbuch, I , Addadi, L, Leiserowitz, L and Lahav, M, J Amer Chem Soc (1988 ) 110 561
7. Weissbuch , I, Frolov, F, Addadi, L, Leiserowitz, L and Lahav, M, J Amer Chem Soc (1990) 110 561
8. Landau, E M, Levanon, M, Leiserowitz, L, Lahav, M and Sagiv, J, Nature (1985) 318 353
9. Landau, E M, Wolf-Grayer, S, Levanon, M, Leiserowitz, L, Lahav, M and Sagiv, J, J Amer Chem Soc (1989) 111 1436
10. Wolf-Grayer, S, Leiserowitz, L, Lahav, M, Deutsch, M, Kjaer, K and Als-Nielsen, J, Nature (1987) 328 63
11. Wolf-Grayer, S, Deutsch, M, Landau, E M, Lahav, M, Leiserowitz, L, Kjaer, K and Als-Nielsen, J, Science (1988) 242 128
12. Jacquemain, D, Wolf-Grayer, S, Leveiller, F, Lahav, M, Leiserowitz, L, Deutsch, M, Kjaer, K and Als-Nielsen, J, J Amer Chem Soc (1990) 112 7724
13. Jacquemain, D, Leveiller, F, Weinbach, S P, Lahav, M, Leiserowitz, L, Kjaer, K and Als-Nielsen, J, J Amer Chem Soc (1990) submitted.
14. Landau, E M, Popovitz-Biro, R, Levanon, M, Leiserowitz, L, Lahav, M and Sagiv, J, Mol Cryst Liq Cryst (1986) 134 323
15. Gavish, M, Popovitz, R, Lahav, M and Leiserowitz, L, Science (1990) 250 973
16. Barton, S W, Thomas, B N, Flow, E B, Rice, S A, Lin, B, Peng, J B, Ketterson, J B and Dutta, P, J Chem Phys (1988) 89 2257
17. Weissbuch, I, Berkovic, G, Leiserowitz, L and Lahav, M, J Amer Chem Soc (1990) 112 5874
18. Zbaida, D, Weissbuch, I, Shavit-Gati, E, Addadi, L, Leiserowitz, L and Lahav, M, Reactive Polymers (1987) 6 241
19. Albeck S, M.Sc. Thesis, Feinberg Graduate School, Rehovot, Israel, (1988)
20. Staab, E, Addadi, L, Leiserowitz, L and Lahav, M, Adv Materials (1990) 2 40
21. Leveiller, F, Jacquemain, D, Lahav, M, Leiserowitz, L, Deutsch, M, Kjaer, K and Als-Nielsen, J, (1990) Science, submitted